Formation of Microporous Membrane of Isotactic Polypropylene in Dibutyl Phthalate-Soybean Oil via Thermally Induced Phase Separation

Gang Chen, Yakai Lin, Xiaolin Wang

Department of Chemical Engineering, Tsinghua University, Beijing 100084, People's Republic of China

Received 10 October 2006; accepted 11 December 2006
DOI 10.1002/app.26406
Published online 1 May 2007 in Wiley InterScience (www.interscience.wiley.com).

ABSTRACT: Isotactic polypropylene (iPP) microporous membranes were prepared via the thermally induced phase separation (TIPS) process with the diluents being dibutyl phthalate (DBP) and soybean oil mixture. By changing the weight ratio of DBP to soybean oil systematically, it was determined experimentally that the cloud-point curves were influenced to a great extent, while the crystallization curves showed much less dependence on the diluents composition. Scanning electron microscopy (SEM) showed that the resulting membrane morphologies changed significantly by varying the composition of the diluents, i.e., by changing the interaction parameter and other characteristics of diluents, the interwoven or celluar structure can be fabricated successfully at a fixed polymer concentration under the same cooling conditions. Different growth rates of iPP spherulite were obtained in the diluents with different composition. It is shown that the spherulites growth rates may be also attributed to the great variations of the final microporous morphology to a certain extent. © 2007 Wiley Periodicals, Inc. J Appl Polym Sci 105: 2000–2007, 2007

Key words: microporous membrane; thermally induced phase separation; isotactic polypropylene; dibutyl phthalate; soybean oil

INTRODUCTION

The thermally induced phase separation (TIPS) method was first introduced by Castro[1,2] in the late 1970s and early 1980s. The basic idea behind this technique is to utilize heat as a latent solvent. By lowering the temperature of an appropriate polymer-diluents system, phase separation can be induced, i.e., a transition from a one-phase homogeneous solution to a two-phase heterogeneous system. This method has been reported to allow for better process control, higher reproducibility, and production of higher void volume (over 60%) compared with the phase inversion method.

As a kind of semicrystalline polymer, different polypropylene-diluent systems were widely used in TIPS process.[3–5] Lloyd and coworkers[6–13] illustrated the TIPS mechanisms and investigated the influence of cooling condition, thermodynamic interaction, characteristics of diluent, crystallization kinetics, and nucleating agent on the membrane morphology. Matsuyama and coworkers[14] prepared asymmetric Isotactic polypropylene (iPP) microporous membranes by inducing a polymer concentration gradient in the polymer-diluents solution prior to phase separation, and investigated the effect of iPP molecular weight and diluent on microporous morphology.[15,16] Most of the interest was focused on the polymer solutions with single diluent; however, few works[17,18] on the systems with mixed diluents were reported.

Both soybean oil and (dibutyl phthalate) DBP can serve as the diluent of iPP with low price and toxicity. However, the iPP microporous membrane prepared in soybean oil owns a poor material strength, while those prepared in DBP showed enclosed pore structure.[19] Therefore, soybean oil or DBP alone is not the appropriate diluent for preparing iPP microporous membrane via TIPS.

In this article, by varying the weight fraction of DBP in the mixed diluents systematically, iPP microporous membranes with various morphology were obtained at a fixed polymer concentration under the same cooling conditions via TIPS. The overall purpose of this research is to investigate the effect of the mixed diluent composition on the membrane morphology and iPP crystallization behavior from the view points of phase separation driving forces and characteristics of diluent.

EXPERIMENTAL

Materials

iPP used in this investigation was commercial grade, (T30S, SinoPec Qilu Company, MFR = 4.38 g/10 min).

Correspondence to: X. Wang (xl-wang@tsinghua.edu.cn).
Contract grant sponsor: National Basic Research Program of China; contract grant number: 2003CB615701.
Contract grant sponsor: Key-Project of Beijing Municipal Education Commission; contract grant number: CXY100030402.

TABLE I
Viscosities of Diluents With Different Weight Ratio of DBP to Soybean Oil

$W_{DBP}/(W_{DBP} + W_{soybean\ oil})$ (%)	100	90	80	70	60	50	40	30	20	10	0
Viscosity (cP)	21	26	27	35	39	43	44	46	57	60	64

Soybean oil without antioxidant was bought in the local supermarket. DBP, *n*-hexane and methanol were analytical grade and used without further purification.

Sample preparation

In practical applications, the polymer concentration is always at around 30 wt % to acquire a balance between porosity and material strength, so the polymer weight fraction applied in this study was fixed at 30 wt %. The polymer and diluent were mixed in a test tube, which was purged with Argon and sealed under flame to prevent oxidation. The sealed test tube was placed in an oven at 453 K for 48 h to yield a homogeneous solution. Scrapped the tube and quenched into water at 303 K for 5 min followed by quenching it into the liquid nitrogen. The diluent remained in the membrane was extracted by *n*-hexane and methanol alternatively for 24 h and dried in a vacuum oven for 12 h.

Phase diagram and sperulite growth rate of iPP

Cloud points and spherulite growth rate for iPP-diluent systems were determined as follows. A small amount of the sample was sandwiched between two glass microscope coverslides with vacuum grease around to limit diluent evaporation during the course of experiment. The sample was heated on a hot stage (THMS600, Linkam Scientific Instruments) at 453 K for 5 min and cooled to 373 K at a controlled rate of 1 K/min for cloud points and 2 K/min for spherulite growth recording. The temperature of the stage was manipulated by a Linksys32 controller. Cloud points were determined visually by noting the appearance of turbidity under an optical microscope (BX52, Olympus Optical). Record the spherulite growth process from the first appearance of the crystal nuclei, and measure the radius every 10 s.

A DSC (DSC 2910, TA Instruments) was used to determine the dynamic crystallization temperature. The solid sample was sealed in an aluminum DSC pan, melted to 453 K, and kept for 10 min to eliminate thermal history, then cooled to 355 K at 5 K/min. The crystallization temperatures were taken as the peak temperature of the resulting exothermal curves.

Scanning electron microscopy observation

For SEM observation, the resulting iPP microporous membranes were fractured in liquid nitrogen and coated with platinum. A SEM (JSM7401, JEOL) with the accelerating voltage set to 1.0 kV was used to examine the morphologies of membrane surfaces and cross sections.

Viscosities of diluent measurement

The viscosities of the diluent were measured in a spinning viscometer (NDJ-8S, Shanghai Precision and Scientific Instrument) in ambient temperature. The viscosities of diluent with different weight fraction of DBP in the diluent were given in Table I.

Soybean oil composition analysis

For soybean oil is a mixture with several kinds of glycerol ester, so the first step was to determine its compositions to calculate the solubility parameter. The compositions of soybean oil were determined via interesterification reaction and gas chromatograph (see Ref. 20). As the fatty acid chains are distributed randomly in the glycerol esters, the compositions of soybean oil can be simplified for the convenience of solubility parameters calculation. The compositions of simplified soybean oil and the corresponding solubility parameters were listed in Table II.

Tensile strength measurement

The membrane was punched into the dumb-bell shape for the tensile test. A universal testing machine

TABLE II
Compositions of the Simplified Soybean Oil and Solubility Parameters

	Tri-linolenic acid glycerol ester	*Tri*-palmitic acid glycerol ester	*Tri*-oleic acid glycerol ester	*Tri*-linoleic acid glycerol ester	*Tri*-stearic acid glycerol ester
δ (MPa^{-1})	18.10	17.37	17.21	17.06	16.90
Volume Fraction (%)	10.99	4.29	22.75	53.43	8.54

TABLE III
Solubility Parameters of Mixed Diluents

$W_{DBP}/(W_{DBP} + W_{soybean\ oil})$ (%)	100	90	80	70	60	50	40	30	20	10	0
δ	19.00	18.93	18.86	18.77	18.67	18.54	18.39	18.2	17.96	17.64	17.20

(AGS-100A, Shimadzu) equipped with a 5 kg load cell conducted the strength measurement. The cross head speed was controlled at 25 mm/min. Average values of the tensile strength was calculated by measuring samples for each batch of product.

RESULTS AND DISCUSSION

Phase diagram

As shown in Table III, when the weight fraction of DBP in the diluent is 100%, the difference in the solubility parameters between iPP ($\delta = 17.5$) and diluents achieved the largest, on the contrary 10% the smallest. As the cloud point measurements were time-consuming and our investigations had little relationship with the cloud-point curves, we only measured the cloud points of iPP-diluent systems with the weight fractions of DBP in the diluent being 10 and 100% experimentally. The cloud-point curves of the other nine samples should be located between those of the above two samples, for higher compatibility between polymer and diluent induces the shift of cloud-point curve to the lower temperature.

Flory[21] gave out the expressions relating the free energy of the polymer-diluent system to the volume fractions of the species. Phase separation results in the formation of two coexistence phases with different polymer fractions. Equating polymer chemical potentials in the polymer-rich and polymer-lean phases, the following two equations describing the binodal or coexistence curve can be obtained.

$$\left[\left(\phi_2^\beta\right)^2 - \left(\phi_2^\alpha\right)^2\right]\chi_1 = \ln\left(\frac{1-\phi_2^\alpha}{1-\phi_2^\beta}\right) + \left(1-\frac{1}{x}\right) \times \left(\phi_2^\alpha - \phi_2^\beta\right) \quad (1)$$

and

$$\chi\left[\left(1-\phi_2^\beta\right)^2 - \left(1-\phi_2^\alpha\right)^2\right]\chi_1 = \ln\left(\frac{\phi_2^\alpha}{\phi_2^\beta}\right) + (\chi-1) \times \left(\phi_2^\alpha - \phi_2^\beta\right) \quad (2)$$

Where ϕ_2^α and ϕ_2^β are the volume fractions of the polymer in phase α and β, respectively, χ_1 is the interaction parameter, x is the ratio of the polymer molar volume to the diluent molar volume.

As to the phase diagram for a mono-disperse polymer-diluent system, the cloud-point curve agrees well with the binodal curve. However, this is not necessarily the case for the polydisperse samples investigated in this experiment. Although the cloud-point curve and the binodal curve may differ somewhat for this system, we still assumed that they were identical. Our qualitative conclusions will not be affected by this assumption.

Figure 1 showed the phase diagram of the polymer-diluent systems with the weight fractions of DBP in the diluent being 100 and 10%. As shown in Figure 1, the cloud-point curves were influenced by the interaction parameters to a great extent, i.e., the weight fraction of DBP to soybean oil in the mixed diluents in our experiments. On the whole, the crystallization temperatures were lowered with the increasing of diluent fraction, whereas the crystallization curves showed much less dependence on the composition of diluent, which agreed with the results reported previously.[16,22] This means that the interaction parameter had little effects on the crystallization temperatures over much of the phase diagram,[23] despite of the great changes in the relative importance of the liquid–liquid phase separation.

The crystallization curve inside the liquid–liquid phase envelope should be remained constant according to the phase rule, which is the characteristic of crystalline phase formed after liquid–liquid separation.[22] However, it is observed that there was an obvious deviation of the crystallization temperatures from the horizontal line in this region. This phenom-

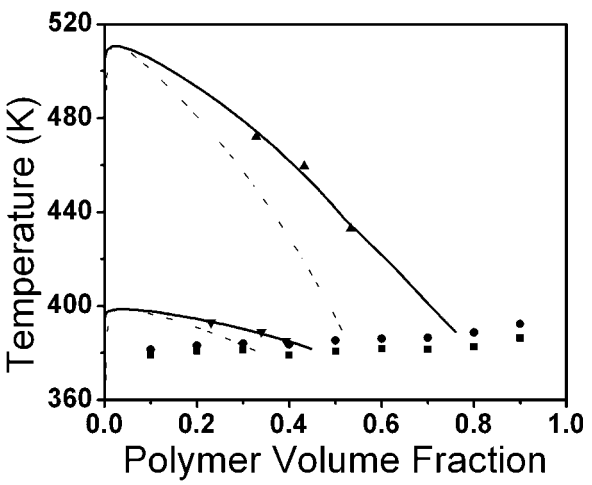

Figure 1 Phase diagram for iPP-diluent systems: cloud points for (▲) $W_{DBP}/(W_{DBP} + W_{soybean\ oil}) = 100\%$, (▼) $W_{DBP}/(W_{DBP} + W_{soybean\ oil}) = 10\%$, and crystallization temperatures for (●) $W_{DBP}/(W_{DBP} + W_{soybean\ oil}) = 100\%$, (■) $W_{DBP}/(W_{DBP} + W_{soybean\ oil}) = 10\%$.

enon can be explained by the polydispersity of iPP, which was reported previously by Lee and coworkers.[22,24] They held the views that the fractionation effects of iPP during cooling brought about the higher molecular weight fraction's being phase separated from solution preceding the crystallization of the lower molecular weight fraction.

The quenching temperature applied in this experiment was 303 k in water, which is usually used in the engineering application and easily to be actualized. According to the phase diagram in Figure 1, it is known that the quenching temperature was far below the coexistence and crystallization curves. Therefore, when iPP-diluent samples were quenched from the homogeneous state, the sample experienced fast cooling and the time for nucleation and growth phase separation in *meta*-stable region was relatively very short. However, liquid–liquid phase separation may still play an important role in determining the final membrane morphology below the crystallization curve due to the higher nucleation barrier to polymer crystallization.[23] Hence, the membrane morphology was mainly dominated by spinodal decomposition phase separation and crystallization of iPP.

Membrane morphology

Figure 2 showed the cross section views of the membrane from 30 wt % solutions. With DBP weight fraction increasing, the resulting microporous morphology changed from interwoven with the pore size on the order of 0.4–1 μm to cellular structure with the pore size on the order of 1–5 μm gradually. Another feature was that the membrane strength became fragile when the soybean oil fraction exceeded 70 wt % in the mixed diluents, and the membrane owned a much higher strength and favorable toughness when DBP fraction was higher.

As shown in Figure 2, the interconnected morphology with relatively uniform pore size resulted, which meant that spinodal decomposition liquid–liquid phase separation played a significant role during cooling due to fast passing through the *meta*-stable region. With the variation of weight fraction of DBP in the mixed diluents from 10 to 100% systematically, the compatibility between polymer and diluent became poorer as illustrated in Table III. The driving forces for crystallization remained almost constant as illustrated in Figure 1, while the driving forces for liquid–liquid phase separation became greater. Furthermore, the time for spinodal decomposition phase separation is longer for the systems with higher DBP fraction. Therefore, the pores with bigger size were obtained under the identical thermal conditions. As shown in Figure 2(a–e), no obvious iPP spherulite was found when soybean oil fraction was higher, for the molecular of soybean oil can prevent crystallization of iPP efficiently. Therefore, the iPP membranes prepared in diluent with higher soybean oil weight fraction owned poor strength as shown in Figure 3.

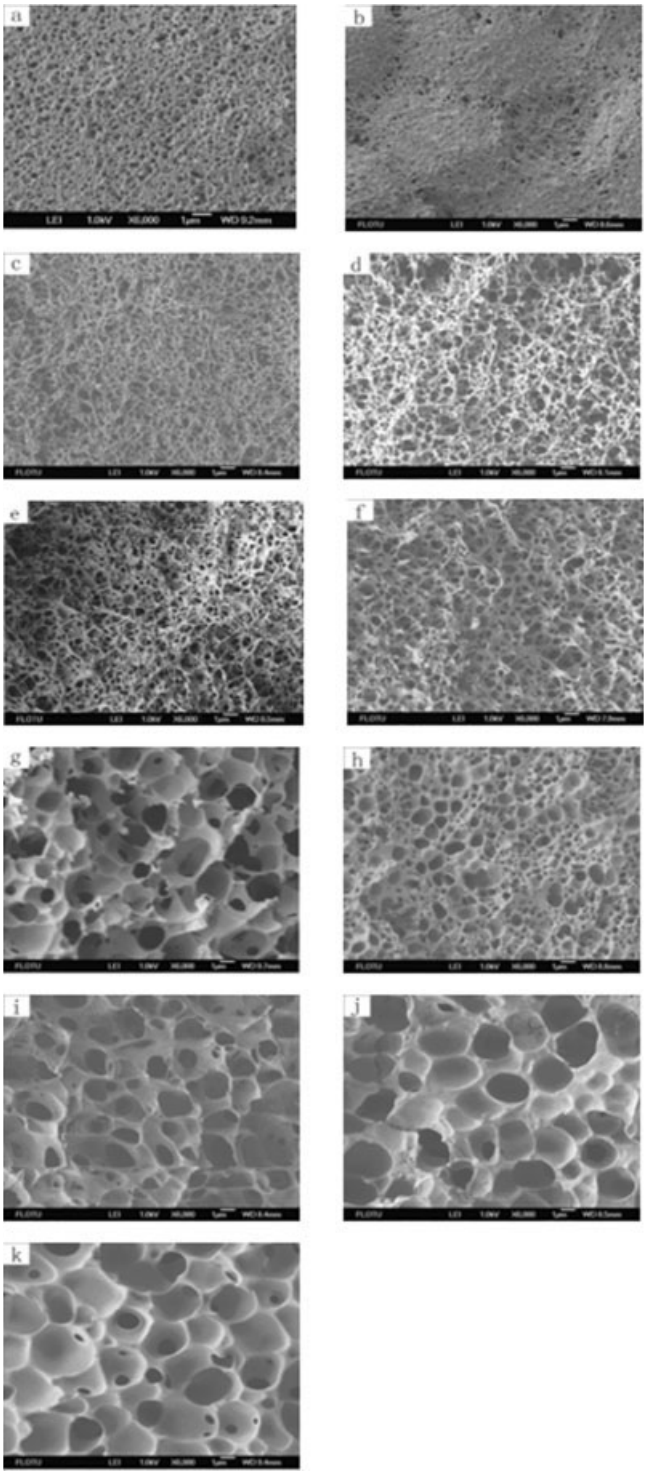

Figure 2 SEM of the cross section of iPP microporous material from 30 wt % solution with the weight ratio of DBP in the diluents being: (a) 0, (b) 10%, (c) 20%, (d) 30%, (e) 40%, (f) 50%, (g) 60%, (h) 70%, (i) 80%, (j) 90%, (k) 100%, respectively. With magnification of 6 k.

What is more, the resulting membrane morphology was influenced by the characteristics of diluent to a

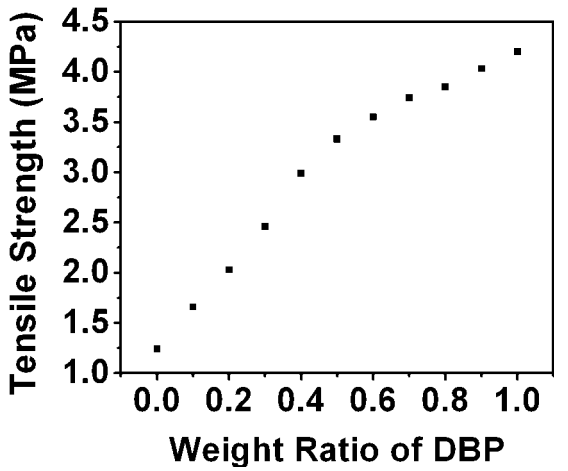

Figure 3 Variation of membrane tensile strength with the weight ratio of DBP in the diluent.

great extent. As the viscosities of mixed diluents shown in Table I, it is known that the viscosity decreased with increasing DBP fraction. Favorable interactions between polymer and diluent induced full extension of iPP chains, which leaded to a higher viscosity of polymer-diluent solution with higher soybean oil fraction, and the *vice versa*. On the other hand, DBP can serve as the plasticizer of iPP, so iPP chains owned a greater mobility when DBP fraction was higher. Therefore, the coarsening process was easily to occur in the systems of higher DBP fraction and the polymer-lean droplets were more easily to be formed, which resulted in bigger pore sizes.

As shown in Figure 2, the interwoven structure was more pervasive in the systems of higher soybean fraction. This difference in morphology was presumably due to the higher viscosity of the polymer solution being able to prevent nucleation and growth liquid–liquid phase separation during quenching more efficiently. Tsai and coworkers[3,25] compared poly (methyl methacrylate) (PMMA)/*tert*-butyl alcohol and PMMA/sulfonlane systems, and they obtained different morphologies under the same conditions owing to different viscosity of the two samples.

In addition to the mentioned two factors, the resulting membrane morphology was influenced by the interfacial tension to a certain extent. With the increasing of DBP fraction in the mixed diluents, the interfacial tension between iPP and diluents increases, which activates the droplet growth of iPP-diluents system. Similar results were reported by Kim and coworkers[26,27] in different systems.

As the iPP microporous membranes were prepared in test tube, the polymer solution had two different cooling conditions, i.e., one surface was contact with water directly and the other one was contact with glass. Therefore, two surfaces with different morphology can be obtained. Figure 4 showed the two surfaces of membrane with weight fraction of DBP in the mixed diluents being 30 and 70% to illustrate the differences between the opposite surfaces. It is obvious that the morphology of the upper surfaces (contact with water directly) was quite different from that of the bottom ones (contact with glass), which may be owing to the constraint of iPP spherulite growth by the glass. The cooling condition in the practical application is more alike as that of the upper surfaces, so the upper surfaces were considered only. As shown in Figure 5, relatively dense surfaces with irregular pore size were obtained when soybean oil fraction was higher, while with the increasing of DBP fraction, typical sieve structure surfaces with uniform pore size on the order of 1–10 μm were resulted and the pore size became lager gradually. The phenomena can also be explained by the mentioned three factors, i.e., compatibility between polymer and diluent, characteristics of diluent and interfacial force of the systems.

iPP sperulite growth rate

Lauritzen and Hoffman (L and H) developed the following growth rate equation for isothermal crystallization.[28]

$$G = G_0 \cdot \exp\left[-\frac{U^*}{R(T_c - T_\infty)}\right] \cdot \exp\left[-\frac{K_g(T_m^0 + T_c)}{2(T_c)^2(T_m^0 - T_c)}\right] \tag{3}$$

Where K_g is the nucleation constant (K^2) and is defined as

$$K_g = \frac{4b_0\sigma\sigma_e T_m^0}{\Delta h_f \kappa} \tag{4}$$

Where

- G is the growth rate to be obtained from thermal optical microscopy (TOM) in μm/min;
- G_0 is the pre-exponentail factor containing quantities not strongly dependent on temperature, in μm/min;
- σ is the lateral surface energy (erg/cm^2)
- σ_e is the fold surface energy (erg/cm^2)
- U^* is a universal constant characteristic of the activation energy of chain motion in the melt
- b_0 is the monolayer thickness (cm)
- R is the gas constant (cal/mol K)
- κ is the Boltzmann constant (erg/K)
- T_m^0 is the equilibrium melting temperature (K)
- T_∞ is the theoretical temperature (K) at which all motion associated with viscous flow or repetition ceases; $T_\infty = T_g - 30$, where T_g is the glass transition temperature of polymer; and
- Δh_f is the heat of fusion (erg/cm^3)

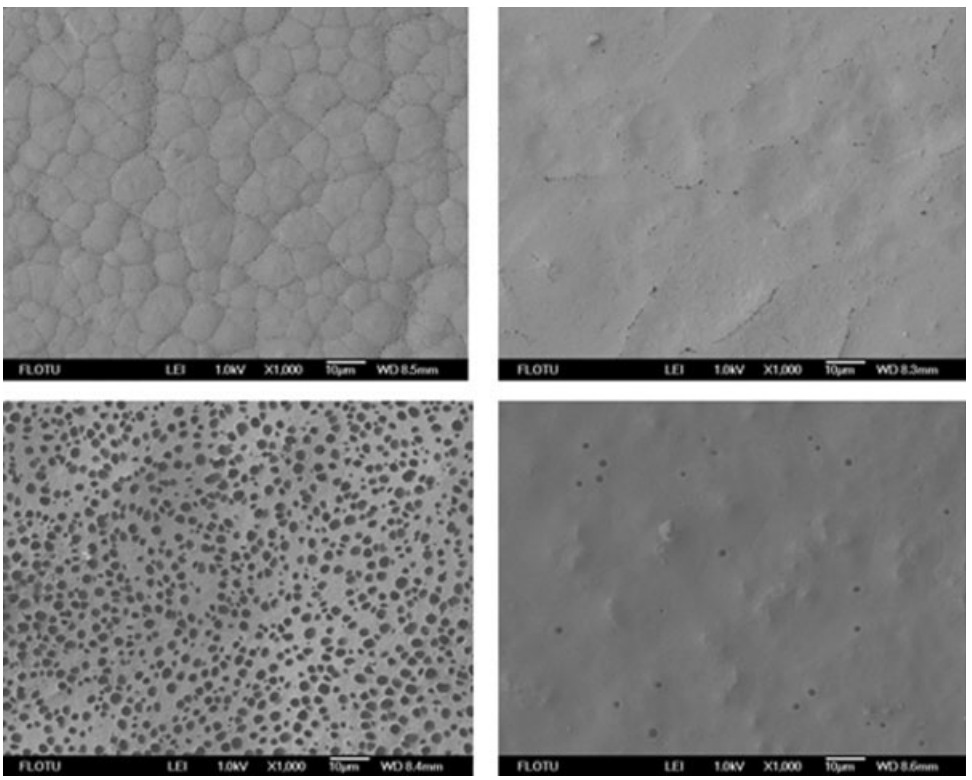

Figure 4 Comparison of the upper surface (contact with water directly) and the bottom surface (contact with glass). Upper: $W_{DBP}/(W_{DBP} + W_{soybean\ oil}) = 30\%$, bottom: $W_{DBP}/(W_{DBP} + W_{soybean\ oil}) = 70\%$, left: upper surface, right: bottom surface

Equation (3) was modified to incorporate the measurement of nonisothermal crystallization data by substituting $(T_m - \alpha T)$ for the crystallization temperature T_c as following.[28]

$$G' = G_0 \cdot \exp\left[-\frac{U^*}{R(T_m - \alpha T) - T_\infty}\right] \times \exp\left[-\frac{K_g(T_m^0 + (T_m - \alpha T))}{2(T_m - \alpha t)^2(T_m^0 - (T_m - \alpha t))}\right] \quad (5)$$

Where

- T_m is defined as the temperature at which the first measurable data is recorded (K); and
- α is the cooling rate (K/min)

In eq. (5), the product $G_0 \cdot \exp[-U^*/R\ (T_m - \alpha T) - T_\infty]$ represents the transportation of polymer segments to the crystallizing site, and $\exp[-K_g(T_m^0 + (T_m - \alpha T))/2(T_m - \alpha t)^2(T_m^0 - (T_m\ - \alpha t))]$ represents nucleation of polymer. With the lowering of crystallization temperature, T_c' the transportation of polymer segments decreased and the nucleation rate increased. Therefore, the overall crystallization rate of polymer increased first and then decreased.

Figure 6 showed the time variation of the spherulite radius R and growth rate G at the cooling rate of 2 K/min. As shown in Figure 6(a), it is known that the spherulite grew with time exponentially. The enlargement of supercooling degree speeded up the crystallization rate, while the addition of diluents brought a negative effect on the spherulite growth. The diluents were rejected from the intraspherulite regions during crystallization and accumulated in the interspherulite regions, which lowered the local polymer concentration and retarded the growth of iPP spherulites physically.[29] As two spherulites approached each other, the volume-filling diluents acted as physical restraint to the growing spherulites. Therefore, the addition of diluents at a fixed crystallization temperature reduced the spherulite growth rate as the spherulites grew. As shown in Figure 6(a), however, the degree of supercooling played an overwhelming role in determining the crystallization rate.

It is also observed that the spherulites growth rate decreased with the increasing of the DBP fraction in the mixed solvents as shown in Figure 6(b). Compared to soybean oil, the interaction between iPP and DBP is poorer. What is more, the viscosity of DBP is smaller than that of soybean oil, so the mobility of DBP molecular is greater. Therefore, with the increasing of DBP fraction, the diluents were more easily to be rejected into the interspherulite regions by the growing spherulites, which retarded the spherulite growth of iPP more efficiently. The tendencies of the spherulite

growth rate further explained the different morphologies of iPP membranes prepared in mixed diluents with different compositions. The relatively slow crystallization rate might enhance the likelihood of the formation of cellular structure before the polymer crystal froze the resulting membrane morphology.

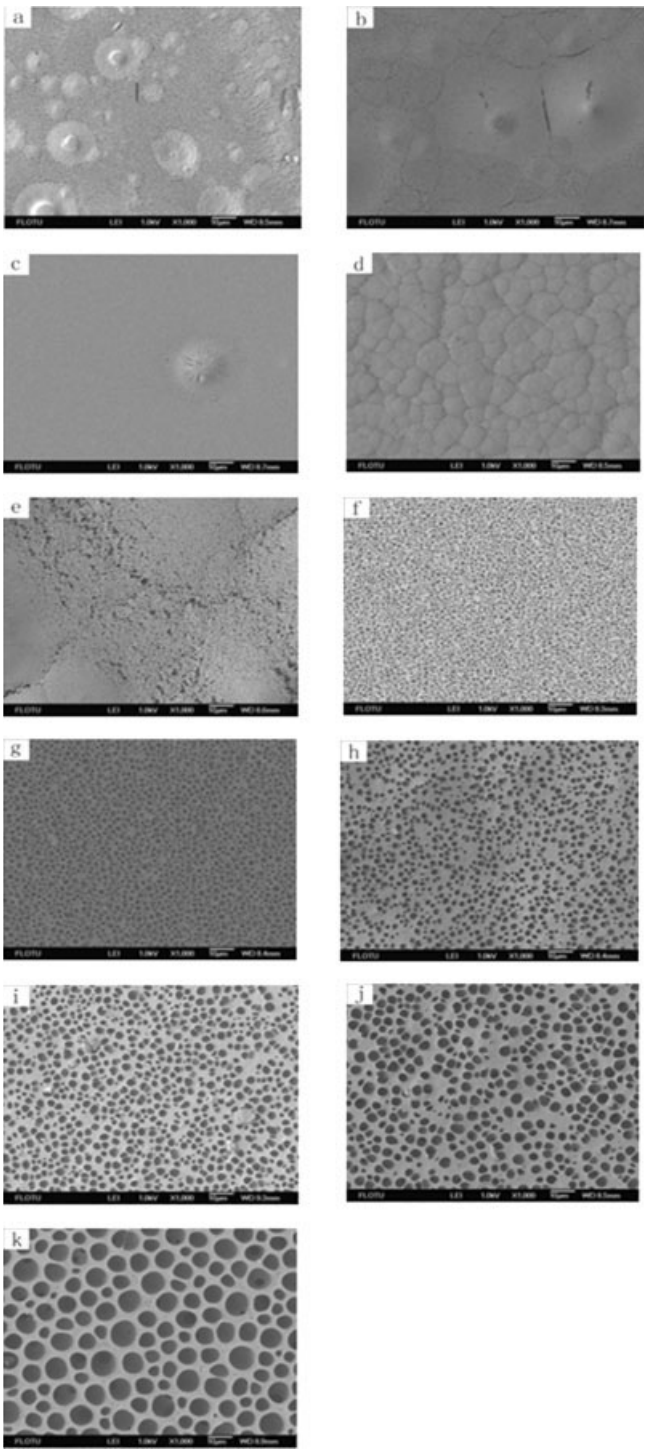

Figure 5 SEM of the upper surfaces of iPP microporous materials from 30 wt % solution with the weight ratio of DBP in the diluents being: (a) 0, (b) 10%, (c) 20%, (d) 30%, (e) 40%, (f) 50%, (g) 60%, (h) 70%, (i) 80%, (j) 90%, (k) 100%, respectively. With the magnification of 1 k.

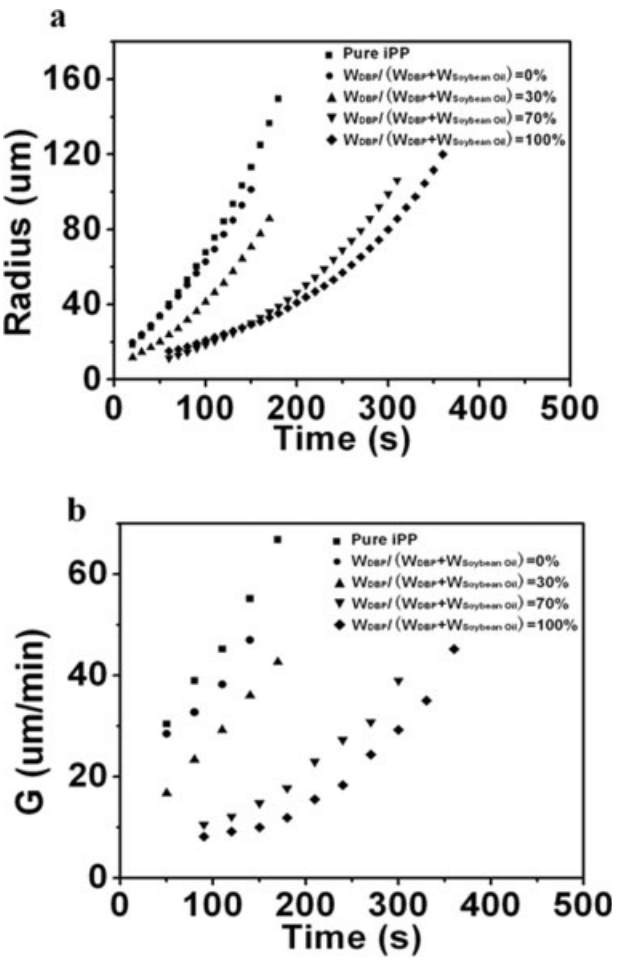

Figure 6 Effect of diluents composition on time variation of (a) spherulite radius and (b) growth rate with the cooling rate at 2 K/min for 30/70 iPP/diluents systems.

CONCLUSIONS

The solvent parameters of mixed diluents were determined. The phase behaviors of iPP/DBP-soybean oil systems were investigated systematically by changing the weight fraction of the two kinds of diluent. The interaction parameters had much less effects on the crystallization curves compared with the cloud-point curves. However, the polydispersity of iPP leaded to an obvious deviation of the crystallization curve from the horizontal line in the liquid–liquid phase separation region. With the increasing of DBP fraction, the cross section of membrane changed from interwoven to cellular structure gradually, and at the same time, relatively dense surfaces with irregular pore size changed to typical sieve structure surfaces with uniform pore size. During cooling, the spherulites grew exponentially with time, and the spherulite growth

rate decreased with the increasing of DBP fraction. The relatively slow spherulite growth rate in the solutions with higher DBP fraction favored the formation of cellular structure with large pore size before iPP crystal locked the resulting morphology.

The further researches on the microporous membrane morphology and crystallization behavior of iPP in mixed diluents are under investigation.

References

1. Castro, A. J. U. S. Pat. 4,247,498 (1981).
2. Young, A. T. Chem Eng News 1978, 56, 23.
3. McGuire, K. S.; Laxminarayan, A.; Lloyd, D. R. Polymer 1995, 3, 4951.
4. Atkinson, P. M.; Lloyd D. R. J Membr Sci 2000, 171, 1.
5. Matsuyama, H.; Berghmans, S.; Lloyd, D. R. Polymer 1999, 40, 2289.
6. Laxminarayan, A.; McGuire, K. S.; Kim, S. S.; Lloyd, D. R. Polymer 1994, 14, 3060.
7. Lloyd, D. R. J Membr Sci 1990, 52, 239.
8. Lloyd, D. R.; Kim, S. S.; Kinzer, K. E. J Membr Sci 1991, 64, 1.
9. Kim, S. S.; Lloyd, D. R.; J Membr Sci 1991, 64, 13.
10. Lim, G. B. A.; Kim, S. S.; Ye, Q.; Wang, Y. F.; Lloyd, D. R. J Membr Sci 1991, 64, 31.
11. Lim, G. B. A.; Kim, S. S.; Ye, Q.; Wang, Y. F.; Lloyd, D R J Membr Sci 1991, 64, 41.
12. Alwattari, A. A.; Lloyd, D. R. J Membr Sci 1991, 64, 55.
13. McGuire, K. S.; Lloyd, D. R.; Lim, G. B.A. J Membr Sci 1993, 79, 27.
14. Matsuyama, H.; Yuasa, M.; Kitamura, Y.; Teramoto, M.; Lloyd, D. R. J Membr Sci 2000, 79, 91.
15. Matsuyama, H.; Maki, T.; Teramoto, M. Asano, K. J Membr Sci 2002, 204, 323.
16. Matsuyama, H.; Teramoto, M.; Kudari, S.; Kitamura, Y. J Appl Polym Sci 2001, 82, 169.
17. Vadalia, H. C.; Lee, H. K.; Myerson, A. S.; Levon, K. J Membr Sci 1994, 89, 37.
18. Yang, Z. S.; Chang, H. Y.; Li, P. L.; Wang, S. C. J Chem Ind Eng (China) 2005, 56, 981.
19. Lotain, G; Yen, L. Y.; Rogers, R. R. U.S. Pat. 4,874,567 (1989).
20. Du, W.; Xu, Y.; Liu, D.; Zeng, J. Mol Catal B: Enzymatic 2004, 30, 125.
21. McGuire, K. S.; Laxminarayan, A.; Lloyd, D. R. Polymer 1994, 35, 4404.
22. Lee, H. K.; Myerson, A. S.; Levon, K. Macromolecules 1992, 25, 4002.
23. Burghardt, W. R. Macromolecules 1989, 22, 2482.
24. Lee, H. K.; Kim, S. C.; Levon, K. J Appl Polym Sci 1998, 70, 849.
25. Tsai, F. J.; Torkelson, J. M. Macromolecules 1990, 23, 4983.
26. Kim, W. K.; Char, K.; Kim, C. K. J Polym Sci: Part B: Polym Phys 2000, 38, 3042.
27. Cha, B. J.; Char, K.; Kim, J. J.; Kim, S. S.; Kim, C. K. J Membr Sci 1995, 108, 219.
28. Hoffman, J. D.; Lauritzen, J. I. J Appl Phys 1973, 44, 4340.
29. Wang, Y. F.; Lloyd, D. R. Polymer 1993, 34, 4740.